IIAT Instituto Internacional de Análise Térmica

Available online at www.bjta.iiatbr.org
Braz. J. Therm. Anal. Vol. 3 No. 1-2 (2014): 11 - 15

Brazilian Journal of Thermal Analysis BJTA

Thermal and spectroscopy characterization of pyridin-2-ylaminomethylene Meldrum´s acid derivatives

L. E. da Silva[1], A. J. Terezo[2], J. A. Teixeira[2], A. B. Siqueira[2*]

[1]*UFPR/Setor Litoral CEP 83260-000, MATINHOS, PR, Brazil.*
[2] *PPGQ - Departamento de Química/ICET/UFMT,CEP 78060-900, Cuiabá, MT, Brazil.*

Received 16/04/2014; accepted 12/05/2014
Available online 26/08/2014

Abstract

Solid compounds of pyridin-2-ylaminomethylene Meldrum's acid derivatives was synthesized and characterized by nuclear magnetic resonance (1H and 13C NMR), mass spectrometry (MS), Infrared spectroscopy (FTIR), simultaneous thermogravimetry-differential thermal analysis (TG-DTA) and differential scanning calorimetry (DSC). The results provided information on the thermal stability and thermal decomposition of the compounds with different substituent groups. The TG-DTA curves show mass losses in two or three steps between 441 - 978 K. The molecular geometry of the compounds was optimized using B3LYP method and 6-311G basis set. The molecular vibration of the optimized compounds was calculated in comparison with the experimental values. The molecular vibration frequencies calculated are generally higher than the corresponding experimental quantities, and it are due to a combination of effects of electronic correlation.

Keywords: thermogravimetry, pyridin-2-ylaminomethylene, spectroscopy

1. Introduction

The thermal studies of heterocyclic organic compounds can be established a correlation with the thermal stability and your composition[1], detection of reversible phase transformations and derivation of new routes of decomposition, which may results in the preparation of different products[2, 3]. The formation of cyclic compounds by pyrolysis of *N*-arylaminomethylene Meldrum´s acid derivatives has been known in solution since 1969 and in the gas-phase since 1983. The precursors can be obtained by reaction of primary aromatic amine with 5-(Methoxymethylene)-2,2-dimethyl-1,3-dioxane-4,6-dione, see Figure 1**,** hence the methodology provides an efficient two-step route to the preparation of a diverse range of heterocyclic compounds such quinolin-4-one [1].

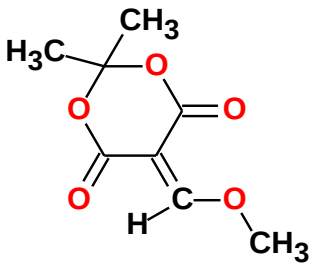

Figure 1: Structure formula of 5-(Methoxymethylene)-2,2-dimethyl-1,3-dioxane-4,6-dione.

The aim of this work is to synthesize a series of pyridylaminomethylene Meldrum´s acid derivatives and characterization of the synthesized compounds by nuclear magnetic resonance (1H and 13C NMR), mass spectrometry (MS), Infrared spectroscopy (FTIR), simultaneous thermogravimetry-differential thermal analysis (TG-DTA) and differential scanning calorimetry (DSC). The structure of adducts allows the loss of a carbon dioxide and ketone molecules to give products of cyclization [4, 5]. The cyclization of 2-aminopyrine derivatives is used for the preparation of 1,8-naphthyridine, but such cyclization types are complicated, due competing reactions at the 3-position of the pyridine ring to give the naphthyridine and ring's nitrogen to form pyrido[1,2-*a*]pyrimidines. The compounds are chemically interesting as they consist of two fused rings. The effect of 6-substituted 2-aminopyridine derivatives on the thermal stability of the ring and rearrangement is also studied in this paper [6]. The thermal decomposition of the adducts is reported to establish relationships between structure and the decomposition process, which were used as synthons for thermolytic-induced heteroelectrocyclic ring closure reactions and in order to estimate the formation of possible region of isomers. The thermal properties of these compounds are important, because it allows information to plan the synthetic chemical reactions conditions.

The experimental infrared spectrum was compared with theoretical infrared spectrum that was realized by *ab initio* calculations. Extensive experimental and theoretical investigations have focused on elucidating the structure and normal vibrations of organic compounds [7]. Thus, calculations of the optimal molecular geometry and vibrational frequency of Pyridin-2-ylaminomethylene Meldrum's acid derivatives were made. It is well known that Hartree-Fock (HF) method tends to overestimate vibrational frequencies. However, density functional theory (DFT) calculations are reported to provide excellent vibrational frequencies of organic compounds, if the calculated frequencies are scaled to compensate for the approximate

*** Corresponding author:** Tel.: +55 (00) 0000-0000
E-mail address: buzutti7@hotmail.com (A. B. Siqueira)

doi: s/n

treatment of electron correlation for basis set deficiencies and the anharmonicity [8].

2. Experimental

2.1. General Procedures

All reactions were conducted in oven or flame dried glassware. Reaction temperatures reported refer to external bath temperatures. All other reagents were used as commercially supplied. Thin Layer Chromatography (TLC) was carried out on E. Merck percolated silica gel 60 F_{254} plates; compounds were visualized using UV radiation (254 nm). Chromatography refers to flash chromatography on E. Merck silica gel 60, 40-60 μm (eluents are given in parentheses).

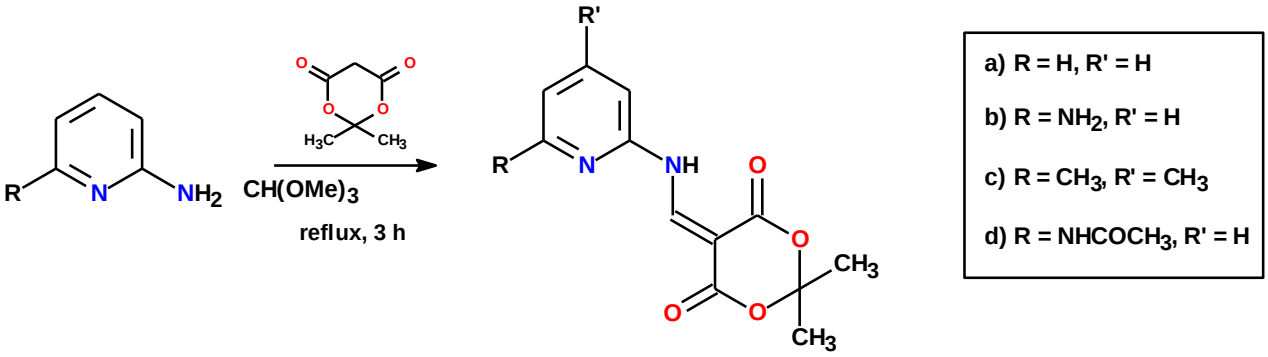

Scheme 1

2.2. General procedure for the synthesis of pyridyl-2-aminomethylene Meldrum's acid derivatives

A solution of Meldrum's acid (30 mmol) in trimethyl orthoformate (50 mL) was refluxed for 3h under N_2, see scheme 1. To this solution the corresponding 2-aminopyridine (30 mmol) was added and the resulting mixture heated at reflux for a further hour. The rotary evaporation followed by recrystallization gave adducts shown below.

***2,2-Dimethyl-5-(pyridin-2-ylaminomethylene)-[1,3]dioxane-4,6-dione*, simplified by LE41 (1a-Scheme 1).** Orange crystalline solid 5.0g (89%): ^{1}H NMR ($CDCl_3$): δ = 1.75 (s, 6H), 7.06 (d, *J* = 8.1 Hz, 1H), 7.19 (t, J^1 = 5.1 Hz, J^2 = 7.00 Hz, 1H), 7.76 (t, *J* = 7.7 Hz, 1H), 8.42 (d, *J* = 5.1 Hz, 1H), 9.41(d, *J* = 13.5, 1H), 11.30 (d, *J* = 13.5, 1H); ^{13}C NMR ($CDCl_3$): δ= 27.54, 89.09, 105.50, 113.28, 121.96, 139.47, 149.47, 149.72, 152.06, 163.59, 166.04. Anal. Calc. for $C_{12}H_{12}N_2O_4$: C = 58.06%; H = 4.87%; N = 11.28%. Found: C = 58.26%; H = 4.86%; N = 11.27%. MS (FAB) 416 ($M^{+\bullet}$), 248 g mol^{-1}.

***5-[(6-Amino-pyridin-2-ylamino)-methylene]-2,2-dimethyl-[1,3]dioxane-4,6-dione*, simplified by LE67 (1b-Scheme 1).** Yellow crystalline solid (62%): R_f 0.57 (EtOAc); IR (nujol): 1675, 1735, 3070 cm^{-1}; ^{1}H NMR ($CDCl_3$, 60 MHz) δ 1.76 (s, 12H), 7.42-7.50 (m, 3H), 8.48 (d, *J* = 15.6 Hz, 1H), 8.52 (d, *J* = 15.6 Hz, 1H), 11.30 (br d, *J* = 15.6 Hz, 1H), 11.50 (br d, *J* = 15.6 Hz, 1H); ^{13}C NMR ($CDCl_3$, 22.4 MHz) δ 27.1, 89.9, 90.2, 105.57, 105.63, 121.1, 122.8, 128.2, 129.6, 132.3, 134.2, 154.3, 155.0, 162.7, 162.8, 165.3; MS (FAB) 451 ($M^{+\bullet}$). Anal. $C_{12}H_{13}N_3O_4$: C = 53.73%; H = 4.47%; N = 15.67%. Found: C = 53.61%; H = 4.74%; N =14.84%.

***5-[(4,6-dimethyl-pyridin-2-ylamino)-methylene]-2,2-dimethyl-[1,3]dioxane-4,6-dione*, simplified by LE06 (1c-Scheme 1).** Colorless crystalline solid (73%): m.p = 183-184°C. IR (KBr): 3264, 3062, 2959, 1700, 1675, 1632, 1555, 1403, 1260, 1020, 914, 821 cm^{-1}. ^{1}H NMR(DMSO-*d6*, 200 MHz) δ 1.75 (s, 6H); 2.33 (s, 3H); 2.47 (s, 3H); 6.65 (s, 1H); 6.85 (s,1H); 9.42 (d, *J* = 13 Hz, 1H) 11.21 (d, *J* = 13 Hz, 1H); 13C RMN (CDCl3, 50 MHz) δ 20.88; 27.02; 23.96; 87.99; 105.00; 110.29; 122.19; 148.52; 150.60; 151.90; 158.33; 163.40; 165.57; 172.33. MS (FAB) 276 ($M^{+\bullet}$). (M+); 172 (100); 200 (30); 146 (45). Anal. Calc. for C14H16N2O4: C = 60.85%; H = 5.83%; N = 10.14%. Found: C = 60.58%; H = 5.81%; N = 10.03%.

***N-{6-[(2,2-Dimethyl-4,6-dioxo-[1,3]dioxan-5-ylidenemethyl)-amino]-pyridin-2-yl}-acetamide*, simplified by LE66 (1d-Scheme 1).** Colorless crystalline solid (71%): (CH_3CN, decomp.); R_f 0.59 (EtOAc); IR (nujol): 1675, 1730, 3170 cm^{-1}; ^{1}H NMR ($CDCl_3$, 60 MHz) δ 1.78 (s, 12H), 2.34 (s, 12H), 7.20 (s, 2H), 8.50 (d, *J* = 13.2 Hz, 2H), 11.33 (br d, *J* = 13.2 Hz, 2H); ^{13}C NMR ($CDCl_3$, 22.4 MHz) δ 19.5, 27.2, 89.0, 105.4, 122.3, 128.7, 137.9, 155.1, 163.2, 165.4; MS (FAB) 444 ($M^{+\bullet}$). Anal. Calc. for $C_{14}H_{15}N_3O_5$: C = 56.56%; H = 5.05%; N = 14.14%. Found: C = 56.08%; H = 5.06%; N = 13.97%.

Infrared spectra of the compounds were performed on a Perkin-Elmer 16 PC-FTIR Instrument with in the 4000-400 cm^{-1} range. The solid samples were pressed into KBr pellets.

TG-DTA and DSC curves were obtained with two thermal analysis systems, model DTG-60H and DSC 60, both from Shimadzu. The purge gas was an air flow of 50 mL min^{-1}. Heating rate of 20 K min^{-1}, alumina and aluminium crucibles, the latter with perforated covers, were used for the TG-DTA and the DSC, respectively.

The 1D – (^{1}H, ^{13}C) NMR experiments were recorded on a Brucker AW-200 spectrometer at 200 MHz (^{1}H) and 50,3 MHz (^{13}C) at 303.15 K and referenced using TMS as internal standard or residual solvent resonances of $CDCl_3$ at δ 7.20 and 77.0, respectively for ^{1}H and ^{13}C NMR.

2.3. General Procedures

In the present investigation, the employed quantum chemical approach to determining the molecular structures was Becke three-parameter hybrid method [9] using the Lee-Yang-Par (LYP) correlation functional[10] and the basis sets used for calculations were the 6-311 G [11, 12]. The performed molecular calculations in this work were done using the Gaussian 03 routine [13, 14].

Theoretical infrared spectrum was calculated using a harmonic Field [15] based on C_1 symmetry (electronic state ^1A). Frequency values (not scaled), relative intensities, assignments and description of vibrational modes are presented. The calculations of vibrational frequencies were also implemented to determine an optimized geometry constitutes minimum or saddle points. The principal infrared-active fundamental modes assignments and descriptions were done by the GaussView 3.0 graphics routine [16].

3. Results and Discussion

3.1. Spectroscopic data

The optimized structures results in theoretically computed energies (a.u.) equals at -874.9925 (LE41), -953.3477 (LE06), -930.3671 (LE67), -1082.6687 (LE66), the representative optimized structure of LE67 is shown in Figure 2. The results are in agreement between experimental IR spectra and theoretical IR ones calculated in B3LYP/6-311 level. The representative experimental and calculated spectra of LE67 are shown in Figure 3.

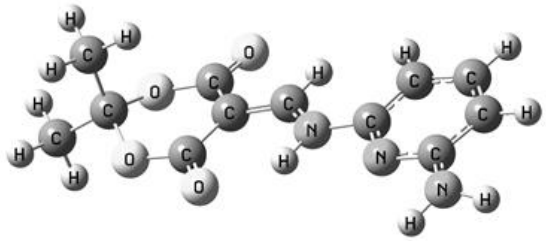

Figure 2: Theoretical 3D structure of solid-state of the LE67 compound using Becke three-parameter hybrid method, 6-311g basis set of Gaussian 03.

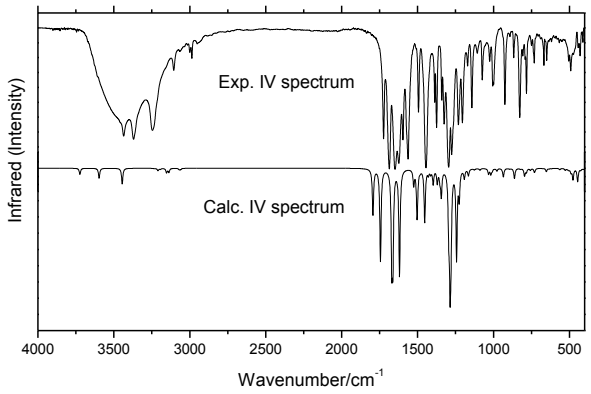

Figure 3: Experimental and calculated IR spectra of LE67.

Different groups of substituents on compounds generate vibrational frequencies characteristics for each group. These differences between the main vibrational assignments are discussed for each group substituent.

R= -H(LE41)

The C=O stretch is a characteristic vibrational frequency of carbonyl group. The band appearing at 1736 cm^{-1} is assigned as C=O stretching vibration in the FTIR spectrum. The theoretically calculated value was 1740 cm^{-1}, showing good agreement with experimental results. The C-C aromatic stretch at 1685 and 1630 cm^{-1} is in excellent agreement with experimental observations at 1670 and 1632 cm^{-1} in the FTIR spectrum.

R= -CH$_3$(LE06)

In the presence of two methyl radicals, the C=O stretching appearing at 1728 and 1682 cm^{-1} for the experimental IR and 1761 and 1714 cm^{-1} for theoretical IR. The peak characteristics of the R(-CH_3) are referents asymmetric out of plane deformation at 1500 cm^{-1} (theoretical) and symmetric out of plane deformation in 1492 cm^{-1} (theoretical) in agreement with the experimental IR in 1556 and 1487 cm^{-1}, respectively. The R (-CH_3) in-plane deformation is observed at 1430 cm^{-1} shows agreement with experimental spectra at 1423 cm^{-1}.

R= -NH$_2$ (LE67)

The mesomeric electron donation from the NH_2 group causes change in the vibrational frequencies of C=O when compared with spectra of LE41. The values to stretch carbonyl of LE67 are 1794 and 1744 cm^{-1} (theoretical) in concordance with experimental values at 1724 and 1686 cm^{-1}. The C–NH_2 out-of-plane bending vibrations at 446 cm^{-1} are also in good agreement with the assignment of the experimental data, 430 cm^{-1}. The NH_2 wagging computed at 476 cm^{-1} is consistent with the amount recorded FTIR 491 cm^{-1}. The NH_2 twisting vibration calculated at 1089 cm^{-1} is very good agreement with the recorded value of 1074 cm^{-1} in FTIR.

R= -NH-CO-CH$_3$ (LE66)

The influence this group is observed in the change of the C=O stretching to 1716 cm^{-1} (theoretical) and 1734 cm^{-1} (experimental) when compared with others. Peaks at 1685 and 1664 cm^{-1} (theoretical) and 1685 and 1621 cm^{-1} (Experimental) are duo to C=O stretches of –NH-CO-CH_3 group. Intense peak at 1521 cm^{-1} are duo to asymmetric stretching of –NCN and in-plane deformation of –CH_3 (substituent group), this values are in concordance with experimental value, 1579 cm^{-1}. The band appearing at 1340 cm^{-1} (theoretical) and 1395 cm^{-1} (experimental) are assigned as -NH-CO-CH_3 stretching.

3.2. TG-DTA and DSC

Simultaneous TG-DTA curves of the compounds show mass losses in two (LE41) and three (LE06, LE67, LE66) steps and thermal events corresponding to these losses or due to physical phenomenon. A great similarity is observed concerning the TG-DTA profiles of these compounds, and they are shown in Figure 4. The thermal behaviour of compounds is strongly dependent on the nature of the substituent group and so the characteristics of each of these compounds will be discussed individually.

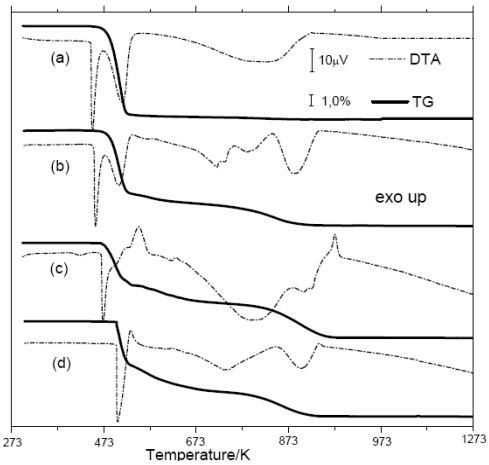

Figure 4: TG-DTA curves of the compounds: (a) LE41 (m = 9.58 mg); (b) LE06 (m = 8.95 mg); (c) LE67 (m = 8.98 mg); (d) LE66 (m = 8.99 mg).

The TG-DTA curve of ***LE41***, see Figure 4(a), shows that the anhydrous compound is stable up to 451 K and above this temperature up to 881 K the thermal decomposition occurs in two steps. The first mass loss that occurs between 451 at 523 K (Δm = 94.47%) corresponding to the endothermic peak at 510 K is attributed to the thermal decomposition. The second mass loss observed between 523 at 881 K (Δm = 5.53%) corresponding to the endotherm between 463 at 923 K is attributed to the final thermal decomposition of the compound. The endothermic peak observed at 448 K without mass loss observed in the TG curve is attributed to melting of the compound and it was confirmed when sample was heated in a tube glass and by DSC curve.

The TG-DTA curve of ***LE06***, see Figure 4(b), shows that thermal decomposition occurs in three steps between 453 and 983 K. The first mass loss occurs between 453 at 523 K with endothermic peak at 505 K is ascribed to the thermal decomposition with loss of 65.78%. The second mass loss that occurs between 523 at 743 K corresponding to the small endothermic peaks at 718 and 736 K occurs with loss of 15.06%. The last step is up to 983 K, with endothermic peak at 883 K and loss of 19.16% is attributed to the final thermal decomposition of the compound without any residue. The endothermic peak observed at 455 K without mass loss observed in the TG curve is attributed to melting of the compound and it was confirmed when sample was heated in a tube glass and by DSC curve.

The TG-DTA curve of ***LE67***, see Figure 4(c), shows that the thermal decomposition of the anhydrous compound occurs in three steps at 473 – 532 K, 532 – 773 K and 773 – 978 K with losses of 43.99%, 21.28% and 34.67 %, respectively. The last two mass losses that begin through a slow process followed by a fast process (532 – 978 K), corresponding to the exothermic peak at 549, 882, 916 and 972 K are attributed to oxidative decomposition. The endothermic peak at 472 K is attributed to the melting of the compound.

The TG-DTA curve of ***LE66***, see Figure 4(d), that the anhydrous compound is stable up to 493 K, this indicates that this compound is more stable in an air atmosphere than the others. The first step of thermal decomposition that occurs through fast process between 493 - 531 K occurs with mass loss of 45.34% corresponding to the an endothermic peak at 503 K and an exothermic one at 530 K are attributed to the thermal decomposition followed by the oxidation of the gaseous products evolved during the thermal decomposition. The last two mass losses between 531 – 769 K (Δm = 28.77%) and 769 – 945 K (Δm = 23.84%) corresponding to the endothermic peaks at 737 K and 900 K and a small exothermic peak at 940 K, attributed to the final thermal decomposition and oxidation of the gaseous products evolved during the thermal decomposition.

The DSC curves of the compounds are shown in Figure 5. A great similarity is also observed in the DSC profiles of LE41 and LE06 compounds; however LE67 and LE66 compounds show peaks characteristic demonstrated in Figure 5. The endothermic peaks at 445 K (LE41) and 450 K (LE06) are attributed to the melting of the compounds. The fusion enthalpy of LE41 and LE06 are 29.12 kJ mol^{-1} and 27.44 kJ mol^{-1}, respectively. The change in the baseline in the DSC curve of the LE67 (356 – 420 K), see Figure 5(c), is attributed to a physical transition of second order.

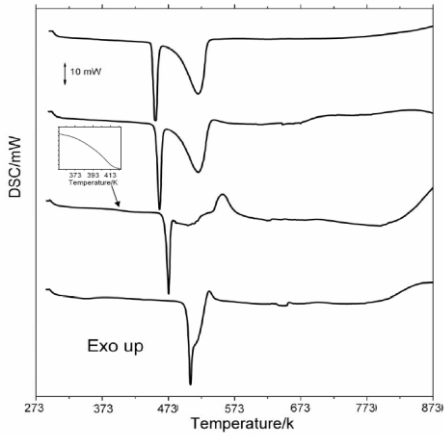

Figure 5: DSC curves of the compounds: (a) LE4; (b) LE06; (c) LE67; (d) LE66).

4. Conclusions

The TG-DTA and DSC provided previously unreported information about the thermal stability, thermal decomposition and physical transformations of these compounds. The thermal stability of these compounds depends on the nature of the substituent group, and it follows the order: LE66 > LE67 > LE06 > LE41. The lower energy (a.u.) calculated for LE41, also showed the lower thermal stability while higher energy calculated for LE66 showed higher thermal stability, too. Theoretical infrared spectra were calculated and compared with experimental data. The difference between the observed and scaled wavenumbers values of most of the fundamentals is very small. Any discrepancy noted between the observed and the calculated frequencies may be due to the fact that the calculations have been actually done on a single molecule contrary to the experimental values recorded in the presence of intermolecular interactions. Therefore, the assignments made at higher levels of theory with only reasonable deviations from the experimental values, seem to be correct.

Acknowledgements

The authors thank Dr. Éder Tadeu Gomes Cavalheiro – IQSC/USP de São Carlos/SP for the computational facilities, CAPES, CNPq and Dr. Valdir Soldi – UFSC.

References

[1] Al-Badri HT, Barbooti MM. Thermoanalytical investigations on heterocyclic organic compounds. Part I. Thermal decomposition of pyrazolinoimides. Thermochim. Acta. 1982:53(1):45-57. [Google Scholar] [Available from] [CrossRef]

[2] Barbooti MM, Al-Badri HT, Roomaya AF. Thermoanalytical investigations on heterocyclic organic compounds. Part II. Thermal decomposition of substituted 1,4-dihydro-2,4-dioxo-2H-3,1-benzoxazine. Thermochim. Acta. 1983:70(1-3):347-358. [Google Scholar] [Available from] [CrossRef]

[3] Al-Badri HT, Abdul-Jalil F, Barbooti MM. Thermoanalytical investigations on heterocyclic organic compounds: Part V: Thermal decomposition of some substituted N-phenylphthalamic acids. Thermochim. Acta. 1989:138(1):13-20. [Google Scholar] [Available from] [CrossRef]

[4] Gaber AEA, McNab H. Synthetic applications of the pyrolysis of Meldrum's acid derivatives. Synthesis. 2001:14:2059-2074. [Google Scholar] [Available from] [CrossRef]

[5] Lorenčak P, Pommelet JC, Chuche J, Wentrup C. A stable methylene ketene and the stepwise fragmentation of Meldrum's acids. J. Chem. Soc. Chem. Comm. 1986:5:369-370. [Google Scholar] [Available from] [CrossRef]

[6] Adams JT, Brasher CK, Breslow DS, Amore ST, Hauser CR. Synthesis of Antimalarials. VI. Synthesis of Certain 1,5- and 1,8-Naphthyridine Derivatives. J. Am. Chem. Soc., 1946:68(7):1317-1319. [Google Scholar] [Available from] [PubMed] [CrossRef]

[7] Kalinowska M, Swislocka R, Lewandowski W. The spectroscopic (FT-IR, FT-Raman, UV and ^{1}H, ^{13}C NMR) and theoretical studies of alkali metal o-methoxybenzoates. J. Mol. Struct. 2006:792-793:130-138. [Google Scholar] [Available from] [CrossRef]

[8] Karabacak M, Cinar M, Kurt M. An experimental and theoretical study of molecular structure and vibrational spectra of 2-chloronicotinic acid by density functional theory and ab initio Hartree–Fock calculations. J. Mol. Struct. 2008:885(1-3):28-35. [Google Scholar] [Available from] [CrossRef]

[9] Becke AD. Density-functional thermochemistry. III. The role of exact exchange. J. Chem. Phys. 1993:98(7):5648-5652. [Google Scholar] [Available from] [CrossRef]

[10] Lee C, Yang W, Parr RG. Development of the Colle-Salvetti correlation-energy formula into a functional of the electron density. Phys. Rev. B. 1988:37(2):785-789. [Google Scholar] [Available from] [CrossRef]

[11] McLean AD, Chandler GS. Contracted Gaussian basis sets for molecular calculations. I. Second row atoms, Z=11–18. J. Chem. Phys. 1980:72(10):5639-5648. [Google Scholar] [Available from] [CrossRef]

[12] Krishnan R, Binkley JS, Seeger R, Pople JA. Self-consistent molecular orbital methods. XX. A basis set for correlated wave functions. J. Chem. Phys. 1980:72(1):650-654. [Google Scholar] [Available from] [CrossRef]

[13] M. J. Frisch, G. W. Trucks, H. B. Schlegel, G. E. Scuseria, M. A. Robb, J. R. Cheeseman, V. G. Zakrzewski, J. A. Montgomery, Jr., R. E. Stratmann, J. C. Burant, S. Dapprich, J. M. Millam, A. D. Daniels, K. N. Kudin, M. C. Strain, O. Farkas, J. Tomasi, V. Barone, M. Cossi, R. Cammi, B. Mennucci, C. Pomelli, C. Adamo, S. Clifford, J. Ochterski, G. A. Petersson, P. Y. Ayala, Q. Cui, K. Morokuma, N. Rega, P. Salvador, J. J. Dannenberg, D. K. Malick, A. D. Rabuck, K. Raghavachari, J. B. Foresman, J. Cioslowski, J. V. Ortiz, A. G. Baboul, B. B. Stefanov, G. Liu, A. Liashenko, P. Piskorz, I. Komaromi, R. Gomperts, R. L. Martin, D. J. Fox, T. Keith, M. A. Al-Laham, C. Y. Peng, A. Nanayakkara, M. Challacombe, P. M. W. Gill, B. Johnson, W. Chen, M. W. Wong, J. L. Andres, C. Gonzalez, M. Head-Gordon, E. S. Replogle, J. A. Pople, Gaussian 03, Revision B.04, Gaussian, Inc., Pittsburgh PA, 2003.

[14] Schlegel, HB. Some practical suggestions for optimizing geometries and locating transition states. in "New Theoretical Concepts for Understanding Organic Reactions", Bertrán J. ed., (Kluwer Academic, the Netherlands), NATO-ASI series C 267, 1989, pg 33-53. [Google Scholar]

[15] Goodson DZ, Sarpal SK, Bopp P, Wolfsberg M. Influence on isotope effect calculations of the method of obtaining force constants from vibrational data. J. Phys. Chem. 1982:869(5):659-663. [Google Scholar] [Available from] [CrossRef]

[16] Dennington II R, Keith TJM, Eppinnett K, Hovell WL, Gilliland R. Semichem. Inc. Shawnee Mission, KS, 2003.